Elsevier Editorial System(tm) for Journal of Proteomics
Manuscript Draft

Manuscript Number: JPROT-D-15-00377R1

Title: Proteomic investigation of whole saliva in Wilson's disease.

Article Type: Full Length Article

Keywords: Wilson's disease.
Human saliva.
Proteomics.
S100A8. S100A9.
α-defensins.
pIgR.
Oxidative stress.
HPLC-ESI-MS.

Corresponding Author: Prof. Tiziana Cabras,

Corresponding Author's Institution:

First Author: Tiziana Cabras

Order of Authors: Tiziana Cabras; Monica Sanna; Barbara Manconi; Daniela Fanni; Luigi Demelia; Orazio Sorbello; Federica Iavarone; Massimo Castagnola; Gavino Faa; Irene Messana

Abstract: Wilson's disease is a rare inherited disorder of copper metabolism, manifesting hepatic, neurological and psychiatric symptoms. Early diagnosis is often unfeasible and a unique diagnostic test is currently inapplicable. We performed the qualitative/quantitative characterization of the salivary proteome/peptidome of 32 Wilson's disease patients by an integrated top-down/bottom-up approach. Patients exhibited significant higher levels of S100A9 and S100A8 proteoforms, and their oxidized forms with respect to controls. Oxidation occurred on methionine and tryptophan residues, and on the unique cysteine residue, in position 42 in S100A8, and 3 in S100A9, that generated glutathionylated, cysteinylated, sulfinic, sulfonic, and disulfide dimeric forms. Wilson's disease patient saliva showed high levels of two new fragments of the polymeric immunoglobulin receptor, and of α-defensins 2 and 4. Level of the whole of the oxidized S100A8 proteoforms correlated with aspartate aminotransferase, and that of glutathionylated S100A9 and α-defensin 4 correlated with hepatic copper content. Overall, the salivary proteome of Wilson's disease patients reflected oxidative stress and inflammatory conditions characteristic of the pathology, highlighting differences that could be useful clues of disease exacerbation.

© <2015>. This manuscript version is made available under the CC-BY-NC-ND 4.0 license https://creativecommons.org/licenses/by-nc-nd/4.0/"

https://dx.doi.org/10.1016/j.jprot.2015.07.033

Dear Editorial Board,

We send to your attention our manuscript titled: "**Proteomic investigation of whole saliva in Wilson's disease.**", by myself, Monica Sanna, Barbara Manconi, Daniela Fanni, Luigi Demelia, Orazio Sorbello, Federica Iavarone, Massimo Castagnola, Gavino Faa and Irene Messana.

The manuscript describes the results obtained through a proteomic study, performed by an integrated top-down/bottom-up platform, on saliva samples from patients suffering of Wilson's disease. This is a pathology characterized by a varied spectrum of manifestations and clinical features and the diagnosis can be reached only by combining several clinical parameters. In our paper, we have highlighted significant quantitative variations in the salivary proteome of WD patients with respect to healthy controls, obtained by an HPLC-ESI-MS label-free quantitation approach. The observed differences, reflecting the oxidative stress and the inflammatory conditions characteristic of WD, could be useful diagnostic clues of disease exacerbation, and they provide suggestions on potential specific, and predictive salivary biomarkers of WD.

Best regards

Sincerely Yours. Tiziana Cabras

Dear Editor,

We have appreciate the comments and suggestions of the reviewer and have, consequently revised the paper (Ref. No.: JPROT-D-15-00377, Title: Proteomic investigation of whole saliva in Wilson's disease). We have applied the following corrections:

R: My major concern goes to the "Correlation analysis with clinical parameters" part that does not contribute strongly to discussion or even to conclusions, it is a little bit confusing regarding the overall manuscript. Why not make it simpler?

- the part concerning the correlation with clinical parameters, as suggested by the Reviewer, was eliminated in order to simplify the paper, and thus we have removed from the manuscript the lines 26-28, Table 1, lines 241-243, lines 375-390, Figure 5, reference 34, lines 445-455, line 486, lines 801-804. Moreover, the paragraph "*Clinical laboratory parametrs.*" In the experimental section, was integrated with the previous "*Ethics Statements and Subjects under Study*."
- Tables and references were re-numbered.

R: There are small mistakes, such as font style/size at pages 305 and 306 and the use of the term "concentrated" in highlights at page 356. I would suggest the use of "higher amount(s)" or similar.

- The whole test of manuscript was re-formatted as Times New Roman 12, and the mistakes of font style/size were corrected. See lines: 287 (Fig. S2A-F), lines 305-306 ((S100A8-SO_2H, 10859.6 ± 0.2 Mmonois., Table 1) was confirmed by MS/MS of the tryptic peptide 37-47 (Table 2 and Fig. S2A-B….), line 308 (…The Mmonois. 10859.6 ± 0.2…).
- We have substitute the term "concentrated" in the line 351 (…hyper-oxidized S100A8 exhibited higher levels in saliva of…) and in the highlights (pIgR peptides, and α-defensin 2 and 4 showed higher amounts in patient's saliva).
- Two sentences were rephrased. Lines 475-476 (…that pIgR itself may be increased in WD patients,…), line 299 (…bottom-up approach allowed confirming S100A8-SO3H and characterizing other…).

Best regards

Sincerely Yours. Tiziana Cabras

Significance

Early diagnosis of Wilson's disease (WD) is often unfeasible and a unique diagnostic test is currently inapplicable. To find suggestions on novel noninvasive markers of WD we performed a pilot study to explore the salivary proteome/peptidome of WD patients by an integrated top-down/bottom-up platform and highlight potential significant qualitative and quantitative variations with respect to healthy controls. WD patient's saliva exhibited an up-regulation of S100A8, S100A9, and their oxidized proteoforms, as well as of pIgR fragments, probably linked to the copper-induced redox unbalance. Also α-defensins 4 was found up-regulated, being this finding probably connected to a metallothionein-involving mechanism that intensifies copper accumulation in WD. Further studies are needed to validate these salivary proteins and peptides as prognostic biomarkers of WD.

*Graphical Abstract

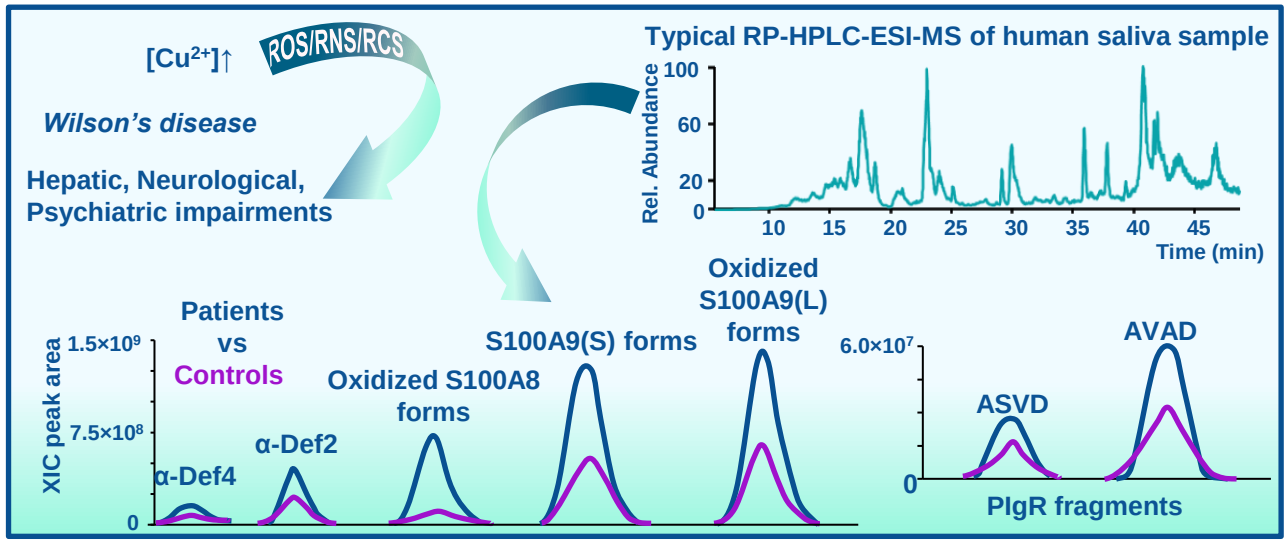

Revised Highlights (for review)

- Saliva proteome of Wilson disease patients and healthy controls showed differences
- Saliva proteome was characterized by an integrated top-down/bottom-up approach
- S100A8, S100A9 and their oxidized forms showed higher levels in patient's saliva
- pIgR peptides, and α-defensin 2 and 4 showed higher amounts in patient's saliva
- Saliva reflects oxidative stress and inflammation conditions of Wilson disease

Revised Manuscript
Click here to download Manuscript: WILSON_SALIVA_revised-20-07.docx Click here to view linked References

Proteomic investigation of whole saliva in Wilson's disease.

Short title: Salivary proteomics of Wilson's disease.

Tiziana Cabras[a*], Monica Sanna[a], Barbara Manconi[a], Daniela Fanni[b], Luigi Demelia[c], Orazio Sorbello[c], Federica Iavarone[d], Massimo Castagnola[de], Gavino Faa[b], Irene Messana[a].

[a]Department of Life and Environmental Sciences, Biomedical section, and [b]Department of Surgery Sciences, and [c]Department of Medical Sciences "M. Aresu", AOU, at University of Cagliari, Monserrato Campus 09042, Monserrato, CA, Italy. [d]Biochemistry and Clinical Biochemistry Institute, Medicine Faculty, Catholic University of Rome, and [e]Institute of Chemistry of the Molecular Recognition CNR, L.go F. Vito 1, 00168 Rome, Italy.

Corresponding author

*Tiziana Cabras PhD

Dipartimento di Scienze della Vita e dell'Ambiente

Università di Cagliari

Cittadella Universitaria di Monserrato

09042 Monserrato (CA) Italy

Tel: +390706754505

E-mail: tcabras@unica.it

Abstract

Wilson's disease is a rare inherited disorder of copper metabolism, manifesting hepatic, neurological and psychiatric symptoms. Early diagnosis is often unfeasible and a unique diagnostic test is currently inapplicable. We performed the qualitative/quantitative characterization of the salivary proteome/peptidome of 32 Wilson's disease patients by an integrated top-down/bottom-up approach. Patients exhibited significant higher levels of S100A9 and S100A8 proteoforms, and their oxidized forms with respect to controls. Oxidation occurred on methionine and tryptophan residues, and on the unique cysteine residue, in position 42 in S100A8, and 3 in S100A9, that generated glutathionylated, cysteinylated, sulfinic, sulfonic, and disulfide dimeric forms. Wilson's disease patient saliva showed high levels of two new fragments of the polymeric immunoglobulin receptor, and of α-defensins 2 and 4. Level of the whole of the oxidized S100A8 proteoforms correlated with aspartate aminotransferase, and that of glutathionylated S100A9 and α-defensin 4 correlated with hepatic copper content. Overall, the salivary proteome of Wilson's disease patients reflected oxidative stress and inflammatory conditions characteristic of the pathology, highlighting differences that could be useful clues of disease exacerbation.

Keywords. Wilson's disease. Human saliva. Proteomics. S100A8. S100A9. α-defensins. pIgR. Oxidative stress. HPLC-ESI-MS.

Introduction.

Wilson's disease (WD) is an autosomal recessive genetic disorder of copper metabolism, characterized by a defective biliary excretion of copper and its failed incorporation into ceruloplasmin, a copper-protein with ferroxidase activity that normally binds 95% of blood copper [1]. The resulting overload of free copper in hepatocytes causes oxidative stress and apoptosis; following the hepatic damage, a massive amount of unbound copper is spilled into the blood and accumulated in other organs, such as brain, hearth, kidney, and cornea, which in turn will be impaired [2]. The pathology is connected to the activity of the transmembrane p-type ATPase called ATP7B. At low or normal copper level, the ATP7B transports copper into the trans Golgi compartment for its incorporation into ceruloplasmin, while at high level, copper is moved towards bile canaliculi to be excreted with the bile [3]. Copper trafficking is interrupted by ATP7B mutations [4]. The most common in the European population is the H1069Q, but over 350 different ATP7B mutations have been identified, and are listed in the Wilson's disease mutation database (http://www.wilsondisease.med.ualberta.ca/database.asp) [5]. The majority of patients are heterozygous, and the distribution of the mutations depends on the population tested [2]. The incidence of the disease is estimated from 1/30000 to 1/100000 with a carrier frequency of 1/90 [6], even if the incidence can vary in different populations, i.e. in Sardinian population the approximate incidence is 1/3000 live births [7]. The WD is a progressive disorder with a broad spectrum of clinical manifestations: hepatic and/or neurological and/or psychiatric that may develop in variable way [2,8,9]. The WD can be lethal when untreated, thus, the early diagnosis is crucial and prevents neurological disability, and liver cirrhosis [10]. A unique diagnostic test for WD is not applicable. The diagnosis is based on the evaluation of different features besides the recognition of typical symptoms, which are often non-specific, and

confusing. The diagnosis, easy in patients with neurological symptoms, is hard in individuals with liver impairments. Decreased serum ceruloplasmin, increased urinary copper excretion, elevated hepatic copper concentration, and serum aminotransferases, and Kayser-Fleischer rings on cornea are considered diagnostic biomarkers of the disease [2,11,12]. Nonetheless, 5-40 % of WD patients exhibit normal ceruloplasmin levels [13], the serum/urine copper levels can be equivocal, and aminotransferase activity cannot reflect the severity of liver injury [2]. In addition, histochemical confirmation of the liver copper content, helpful in diagnosis, requires invasive analyses, and a negative result does not exclude WD [14-16]. *ATP7B* mutation analysis is very advantageous, but systemic genetic testing is not routinely applied in clinical practice due to the many different mutations implicated. The need of novel and unequivocal diagnostic biomarkers has stimulated the research towards proteomics investigations on animals [17-19], *in vitro* WD models [20], and WD human serum [21]. These studies, based on bottom-up proteomic platforms, highlighted altered levels of proteins involved in the oxidative stress. In the present study, whole saliva of a Sardinian cohort of WD patients was investigated by an integrated top-down/bottom-up platform to exploit the peculiarities of each approach and benefit from both. The bottom-up approach is characterized by a high throughput, and it benefits from the availability of bio-informatics tools for automated analysis of MS/MS data. On the other side, the top-down approach allows obtaining structural information and label-free quantifying of intact proteins and their proteoforms, especially the naturally occurring proteolytic peptides. The implementation of both approaches in the present work highlighted qualitative and quantitative variations of proteins, peptides, and modifications correlated to the pathology, and suggested possible salivary biomarkers of the disease.

Material and methods.

Reagents.

All chemicals and reagents were of analytical grade and were purchased from Sigma Aldrich (St. Louis, MI) and Merck (Damstadt, Germany).

*Ethics Statements and Subjects under Study***.**

The study protocol and written consent forms were approved by the Medical Ethics Committee of the Faculty of Medicine of the Catholic University of Rome (according to the instructions of the Declaration of Helsinki). The WD patients were enrolled for the study at the Hepato-Gastroenterology Service of the "Policlinico Universitario Monserrato", Cagliari, Sardinia, Italy. The patients were 32 (mean age ± SD: 42 ± 13; 18 female (F), 14 male (M)), the healthy control (HC) group comprised the same number of subjects (mean age ± SD: 39 ± 14; 19 female (F), 13 male (M)). The WD diagnosis was based on the combination of several criteria: clinical symptoms, Kayser-Fleisher ring, and laboratory tests. Based on clinical manifestations the patients were classified as hepatic (N =23), hepatic/ neurologic (N = 4), hepatic/psychiatric (N = 1), hepatic/neurologic/psychiatric (N = 4). Diagnosis was confirmed by serum ceruloplasmin, total serum copper, cupruria baseline, hepatic parenchymal copper concentration following hepatic ago biopsy. Histological evaluation of grading and staging of liver fibrosis, and molecular biology analysis of the *ATP7B* gene mutations were also carried out.

Sample Collection.

Unstimulated whole saliva was collected according to a standardized protocol. Donors did not eat or drink at least 2 h before the collection, which was performed in the morning between

10:00 A.M. and 12:00 P.M. with a soft plastic aspirator. Saliva was transferred to a plastic tube in an ice bath, and 0.2% 2,2,2-trifluoroacetic acid (TFA) was immediately added in 1:1 v/v ratio. The solution was then centrifuged at 10000 x g for 10 min at 4 °C. The acidic supernatant was separated from the precipitate, and either immediately analyzed by HPLC-ESI-MS (100 µl, corresponding to 50 µl of saliva) or stored at -80° C until the analysis.

Low-resolution HPLC-ESI-IT-MS Experiments.

Search and quantification of peptides and proteins were made by low-resolution reversed phase (RP)-HPLC-ESI-MS analysis of the acid soluble fraction of whole saliva samples. The measurements were carried out by a Surveyor HPLC system connected by a T splitter to a diode-array detector, and to a LCQ Advantage mass spectrometer (ThermoFisher Scientific San Jose, CA). The mass spectrometer was equipped with an ESI source. The chromatographic column was a Vydac (Hesperia, CA) C8 column with 5 µm particle diameter (150 x 2.1 mm). The following solutions were used: (eluent A) 0.056% (v/v) aqueous TFA, and (eluent B) 0.05% (v/v) TFA in acetonitrile-water 80/20. The gradient applied for the analysis of saliva was linear from 0 to 55% of B in 40 min, and from 55% to 100% of B in 10 min, at a flow rate of 0.30 ml/min. The T splitter resulted in a flow-rate of 0.20 ml/min toward the diode array detector, and 0.10 ml/min toward the ESI source. During the first 5 min of separation, the eluate was diverted to waste to avoid instrument damage because of the high salt concentration. The photodiode array detector was set at 214 and 276 nm. Mass spectra were collected every 3 ms in the m/z range 300-2000 in positive ion mode. The MS spray voltage was 5.0 kV, and the capillary temperature was 260 °C. MS resolution was 6000. More information on the MS method is reported in the supplemental file *Low_res_ESI-MS_method*. Experimental mass values were

obtained by deconvolution of averaged ESI-MS spectra automatically performed using MagTran 1.0 software [22].

Characterization of Salivary Peptides and Proteins.

Experimental, and theoretical average mass values (Swiss-Prot Data Bank, http://us.expasy.org/tools) of proteins and peptides characterized by us in previous studies [23-27] and found with levels not statistically different between WD patients and controls are reported in supplemental Table S1. Table 1 reports Swiss-prot code, elution time, experimental (Exp.) and theoretical (Th.) average and monoisotopic mass values of α-defensins, two fragments of Polymeric Immunoglobulin Receptors (pIgR), and S100A8 and S100A9 and their oxidized proteoforms. To characterize the two fragments of pIgR and the oxidized derivatives of S100A8 and S100A9 we applied both a top-down proteomic approach on the intact proteins and peptides present in the acidic supernatant of whole saliva, and a bottom-up approach on the tryptic digests of salivary enriched fractions.

Enriched fraction preparation and trypsin digestion.

Enriched fractions were obtained by preparative RP-HPLC (Dionex Ultimate 3000 instrument, ThermoFisher Scientific, Sunnyvale CA) of pools of WD saliva. The chromatographic column was a reversed phase Vydac (Hesperia, CA) C8 column with 5 µm particle diameter (250 x 10 mm). The solutions used for preparative RP-HPLC were the same utilized for analytical HPLC-ESI-MS experiments. The gradient was linear from 0 to 60% B in 40 minutes and from 60 to 100% B in 5 minutes, with a flow rate of 2.8 ml/min. Four fractions corresponding to peaks eluting between 39 and 44 minutes were collected separately and lyophilized. Each fraction was

solubilized in 100 µl of ultrapure H_2O, and 1/3 of the solution was acidified with 0.2% TFA (1:1 v/v ratio) to be checked by low-resolution HPLC-ESI-MS. The remaining sample was submitted to digestion by the kit "Trypsin Singles Proteomic Grade" (Sigma-Aldrich) according to the manufacturer's instructions. Digestion was stopped after 12 h by acidification with 0.1% TFA (final concentration), and the solution stored at -80° C until the analysis by high-resolution HPLC-ESI-MS/MS.

High-resolution HPLC-ESI-MS/MS experiments.

The experiments were carried out by an Ultimate 3000 Micro HPLC apparatus (ThermoFisher Scientific, Sunnyvale, CA) equipped with a FLM-3000-Flow manager module coupled to a LTQ Orbitrap XL apparatus (ThermoFisher Scientific). The columns were a Zorbax 300SB-C8 column (3.5 µm particle diameter; 1.0 x 150 mm) for the top-down analysis, and a Zorbax 300SB-C18 column (5 µm particle diameter; 1.0 x 150 mm) for the bottom-up. Eluents were: (eluent A) 0.056% (v/v) aqueous TFA, and (eluent B) 0.05% (v/v) TFA in acetonitrile-water 80/20. For both top-down and bottom-up analyses the gradient was: 0–2 min 5% B, 2-40 min from 5% to 55% B (linear), 41-43 min from 55% to 100% B, at a flow rate of 80 µL/min. MS and MS/MS spectra were collected in positive mode using the lock mass for internal mass calibration (polydimethyl cyclosiloxane, 445.1200 m/z) with the resolution of 60000 and 30000, respectively. The m/z range was from 600 to 2000 in the top-down experiments, from 300 to 2000 in the bottom-up experiments. Tuning parameters: capillary temperature was 250 °C, and the source voltage 4.0 kV, capillary voltage and tube lens voltage were 37 V, and 150 V in the top-down; 48 V, and 150 V in the bottom-up experiments. In data-dependent acquisition mode the three most abundant ions were selected and fragmented by using collision-induced

dissociation (CID, 35% normalized collision energy for 30 ms, isolation width of 6–10 *m*/*z*, activation q of 0.25). Detailed instrumental conditions are reported in the supplemental file *High_res_ESI-MS_method*. The inject volume was 20 μL. HPLC-ESI-MS and MS/MS data were generated by Xcalibur 2.2 SP1.48 (Thermo Fisher Scientific) using default parameters of the Xtract program for the deconvolution. MS/MS data were analyzed by the Proteome Discoverer 1.2 program, based on SEQUEST cluster as a search engine (University of Washington, licensed to Thermo Electron Corp., San Jose, CA) against the Swiss-Prot human proteome (September, 2014 released; Swiss Prot human complete.fasta; 47622 non redundant protein sequences). For peptide matching the limits were: Xcorr scores greater than 1.5 for singly charged ions, 2.0 and 2.5 for doubly and triply charged ions, respectively. Furthermore, the cleavage specificity was set to trypsin with two missed cleavages in the bottom-up analysis. Precursor mass search tolerance was 10 ppm and fragment mass tolerance 0.8 Da. Target FDR was: 0.01 (strict), 0.05 (relaxed). The following modifications were searched: phosphorylation, acetylation, oxidation of methionine and tryptophan residues, as well as oxidative cysteine modifications, such as glutathionylation, cisteinylation, nitrosylation, sulfonic, sulfinic, and sulfenic acid. Peptide sequences and sites of covalent modifications were also validated by manual inspection of the experimental fragmentation spectra against the theoretical ones generated by MS-Product software available at the ProteinProspector website (http://prospector.ucsf.edu/prospector/mshome.htm).

Quantification.

The area of the low-resolution RP-HPLC-ESI-MS eXtracted Ion Current (XIC) peaks (signal/noise ratio >5) was used for quantification. The XIC search reveals the peak associated

with the protein of interest by extracting along the total ion current chromatographic profile the intensity of the ion current of specific multiply charged ions generated by the ESI source. The area of the XIC peaks is proportional to the peptide/protein concentration, therefore, under constant analytical conditions, it can be used for a quantitative analysis and comparative studies [28,29]. The estimated percentage error of the XIC procedure was <8%. A window of ± 0.5 Da was used to extract XIC peaks. The ions used to selectively extract and quantify the proteins and peptide, carefully selected to exclude values in common with other co-eluting proteins, are reported in Table 1 and Table S1.

Statistical Analysis.

GraphPad Prism (version 4.0) was used for statistical analysis. Ranges, medians, means, and standard deviations were calculated for XIC peak area of all the peptides and proteins. The following statistical tests were used depending on data distribution (normal or skewed), and variance (homogeneous or unequal): parametric *t* test (variance homogeneous); *t* test with Welch correction (normal distribution, variance unequal), and the nonparametric Mann-Whitney test (skewed distribution, variance unequal).

Results.

The following proteins and peptides were searched and quantified by a top-down proteomic approach in saliva from WD patients: histatins, S-type cystatins, statherin, proline-rich peptide P-B, salivary acidic proline-rich proteins (aPRPs), α-defensins 1–4, cystatins A, B, C, β-thymosins 4 and 10, S100A7 (D27), S100A8, S100A9 (short (S) and long (L) isoforms), S100A12, as well as acetylated, phosphorylated, methionine oxidized proteoforms and oxidative cysteine

modification producs, such as cysteinylated and glutathionylated derivatives. Figure 1 shows a typical chromatographic profile of the acidic soluble fraction of saliva from a WD patient, with the elution range of several salivary proteins/peptides. In this study, we did not evaluate basic proline-rich proteins due to their high variability linked to the physiological status [30,31]. Table 1 and supplemental Table S1 report the Swiss-prot codes, elution times, experimental average (low-resolution) and monoisotopic (high-resolution) mass values (Mav., Mmonois.), and the multiply-charged ions utilized to selectively extract the ion current peaks used to quantify proteins/peptides investigated. In particular, Table 1 reports information concerning peptides and proteins showing quantitative variations between WD patients and healthy controls. In the low resolution HPLC-ESI-MS profiles we also detected several masses not previously characterized by us. These masses were attributed to two naturally occurring fragments of the polymeric immunoglobulin receptor pIgR, and to proteoforms of S100A8 and S100A9 with a different degree of oxidation (Table 1). The structural characterization was based on the high-resolution HPLC-ESI-MS/MS top-down approach directly applied on the acidic soluble fraction of saliva samples and on the bottom up high-resolution HPLC-ESI-MS/MS analysis performed on trypsin digests of enriched fractions obtained by preparative RP-HPLC of pools of WD saliva, as shown in Figure 2 and described in the following sections.

High-resolution top-down structural characterization of pIgR, and three S100A8 oxidized proteoforms.

The structural characterization was performed by high-resolution HPLC-ESI-MS/MS analysis of the naturally occurring peptidome/proteome present in the acidic supernatant of whole saliva from WD patients.

The two peptides eluting in the region 23.4-27.0 min of the low-resolution HPLC-ESI-MS profile of saliva, were identified as the fragment 610-648 (named by us AVAD), and the fragment 623-648 (named ASVD) of pIgR, respectively, (Table 1), on the basis of high-resolution MS/MS performed on triply-charged ion 1278.62 ± 0.02 m/z of AVAD, and on doubly-charged ion 1246.12 ± 0.02 m/z of ASVD. The high-resolution spectra are reported in Fig. S1 of the supplemental **Top-down proteomics characterization** file.

S100A8 oxidation involved methionine 1 and 78 (M1, M78), tryptophan 54 (W54), and cysteine 42 (C42) (Table 1). Three proteoforms of S100A8 showed C42 oxidized to sulfonic acid (S100A8-SO_3H). The first showed a further oxidation at W54 (S100A8-SO_3H/W54ox). The other two forms were isobaric derivatives of S100A8-SO_3H; one form was also oxidized at W54 and M78 (S100A8-SO_3H/W54ox/M78ox), the other was dioxidized at W54 (S100A8-SO_3H/W54diox). These proteoforms hereafter will be named hyper-oxidized S100A8 (Table 1). Top-down high-resolution MS/MS annotated spectra of intact S100A8-SO_3H/W54ox and hyper-oxidized S100A8 forms are respectively shown in Fig. S2A-F, and S3A-E of the supplemental **Top-down proteomics characterization** file. The neutral loss of H_2SO_3 (81.97 Da) [32] observed for S100A8-SO_3H/W54ox and only for S100A8-SO_3H/W54ox/M78ox was in agreement with the presence of the sulfonic acid residue, and MS/MS data of the ion 910.56 m/z ($[M+12H]^{+12}$) confirmed the structures of the two co-eluting and isobaric hyper-oxidized S100A8 proteoforms (Fig. S3A-E).

High-resolution bottom-up structural characterization of S100A8, S100A9 oxidized proteoforms.

Enriched fractions of S100A8, S100A9 and their oxidized proteoforms obtained by preparative RP-HPLC of pools of patient saliva were digested with trypsin and digests analyzed by high-

resolution HPLC-ESI-MS/MS. All the MS/MS annotated spectra are reported in the supplemental files **Bottom-up oxidized S100A8-S100A9** and **Bottom-up unmodified S100A8-S100A9**. The bottom-up approach allowed confirming S100A8-SO3H and characterizing other oxidized derivatives of S100A8.

MS/MS sequencing of the tryptic peptides with monoisotopic $[M+H]^+$ 1412.68 ± 0.02, and 1540.77 ± 0.03 m/z corresponding to S100A8-SO_3H fragments 37-47, 37-48, and 36-47 (the latter two isobaric) confirmed the sulfonic acid modification of C42 (Table 2 and Fig. S1A-C of the **Bottom-up oxidized S100A8-S100A9** file).

One proteoform of S100A8 with C42 oxidized to sulfinic acid (S100A8-SO_2H, 10859.6 ± 0.2 Mmonois., Table 1) was confirmed by MS/MS of the tryptic peptide 37-47 (Table 2 and Fig. S2A-B of the **Bottom-up oxidized S100A8-S100A9** file) which showed the characteristic neutral loss of H_2SO_2 (65.98 Da) [33]. The Mmonois. 10859.6 ± 0.2 could be also in agreement with dioxidized derivatives of S100A8, i.e. at W54 and M1, or M78 and M1, or W54 and M78. This possibility could not be excluded nor confirmed by high-resolution MS/MS due to the separation of the modification sites in the tryptic peptides (Table 2). Indeed, oxidation of M1 in S100A8 was evidenced by MS/MS data of the tryptic peptide 1-23 (Table 2 and Fig S3 of the **Bottom-up oxidized S100A8-S100A9** file). Furthermore, masses attributable to tryptic peptides oxidized at M78 and W54, but not confirmed by MS/MS due to the low intensity, were also detected. The tentative attributions and monoisotopic $[M+H]^+$ m/z values were: fragment 78-84 of S100A8- M78ox, with m/z 729.32 ± 0.01 (theor. 729.38) eluting at 20.7 min; fragment 50-56 of S100A8-W54ox, with m/z 838.35 ± 0.01 (theor. 838.41, 20.7 min); fragment 48-56 of S100A8-W54ox, with m/z 1110.47 ± 0.02 (theor. 1110.59, 22.0 min).

Glutathionylation of C42 in S100A8 (S100A8-SSG, Table 1) was demonstrated by MS/MS data of the 37-47 glutathionylated peptide (monoisotopic monocharged ion with m/z 1669.76 ± 0.03, Table 2). The Figure 3A shows the high-resolution MS/MS of the triply-charged ion with m/z 557.26 with the characteristic neutral loss of pyroglutamate (129.04 Da), that confirmed the presence of the glutathionyl moiety. The monoisotopic mono-charged ions with m/z 1649.78 ± 0.03 and 1393.73 ± 0.02 were tentatively attributed to the following fragments of C42-nitrosylated S100A8 (S100A8-SNO, Table 1): 37-49 (or 36-48) fragment (theor. 1649.87 m/z) and 37-47 fragment (theor. 1393.68 m/z).

Cysteine 42 of S100A8 originated also a disulfide bridge with cysteine 3 of S100A9(L) (S100A8/A9-SSdimer, Table 1). The presence in saliva of WD patients of this covalent hetero-dimer was confirmed by high-resolution MS/MS of the monoisotopic doubly-charged ion with m/z 877.93 ± 0.01, attributed to the tryptic peptide in which fragment 2-4 of S100A9(L) was linked to fragment 37-47 of S100A8 (Fig. 3B, Table 2). The monoisotopic mono-charged ion with m/z 2628.26 ± 0.04 was attributed to fragment 2-10 of S100A9(L) linked to fragment 36-47 of S100A8, but not confirmed by MS/MS data due to its low abundance. The two peptides, with the following experimental monoisotopic $[M+H]^+$ m/z values: 784.49 ± 0.01 and 1528.72 ± 0.03 were tentatively attributed to Nα-Ac-TCK dimer (theor. 784.36 m/z), and Nα-Ac-TCK bound to Nα-Ac-TCKMSQLER (theor. 1528.72 m/z), respectively, generated by S100A9(L)-SSdimer (Table 1).

Both the short and the long glutathionylated S100A9 proteoforms were detected as mono-oxidized derivatives on one of the following methionine residues: M59 (or M63), M77 (or M81), M79 (or M83), and M90 (or M94) (Table 1), as confirmed by high-resolution MS/MS of the

mono-oxidized tryptic peptides reported on Table 2, and Fig. S4A-E of the **Bottom-up oxidized S100A8-S100A9** file.

Salivary protein quantification and statistical analysis.

By comparing the WD group with the HC group none differences were found in the levels of proteins and peptides secreted by salivary glands, such as histatins, statherin, P-B peptide, cystatins S, and C, and aPRPs, as well as in the level of cystatin A, and B. Conversely, saliva of WD patients with respect to HC subjects showed significant higher levels of AVAD and ASVD pIgR peptides, and α-defensins 2 and 4, the main differences being exhibited by AVAD ($p = 0.003$), and α-defensin 4 ($p = 0.004$) (Table 3, Figure 4A-B).

Moreover, S100A9(S), S100A9(L)-SSG, and their phosphorylated derivatives, S100A8 and hyper-oxidized S100A8 exhibited higher levels in saliva of WD patients with respect to HC subjects (Table 3, Figure 4C-D). Statistical analysis was performed considering the totality of non-phosphorylated and phosphorylated forms of short and long S100A9 and the results are reported in Table 3. WD patients showed higher levels and frequencies of S100A8-SO_3H/W54ox, S100A9(L)-SSC, S100A9(L)-SSC phosphorylated, S100A9(S)-Mox and S100A9(S)-Mox phosphorylated with respect to controls, even though without a statistical significance (Table 3). In WD patients with high concentration of S100A8 and S100A9, also the following modifications were detected, even if sporadically: S100A8-SSG and S100A8-SNO in 5 patients; S100A8-SO_2H in 3 patients, S100A8/A9-SSdimer and S100A9(L)-SSdimer in 8 patients (Table 3). In 8 WD patients S100A8 was detected only in the oxidized forms. Statistical

analysis highlighted significant higher levels in WD patients with respect to HC subjects of the totality of the oxidized proteoforms of S100A8 (S100A8ox tot), and the totality of the oxidized proteoforms of S100A9(L) (S100A9(L)ox tot) (Table 3, Figure 4E). A calculation of the relative abundance of the different proteoforms revealed that S100A8 was mainly represented by its oxidized derivatives in saliva of both WD patients and controls: 75 ± 30% in WD patients, 77 ± 42% in HC subjects. Among the oxidized proteoforms the most abundant was the hyper-oxidized S100A8 (WD 42 ± 40%, HC 59 ± 46%), followed by S100A8-SO_3H/W54ox (WD 12 ± 23%, HC 18 ± 32%), S100A8/A9-SSdimer (WD 11 ± 27%), S100A8-SNO (WD 8 ± 22%), S100A8-SSG (WD 1 ± 3%), and S100A8-SO_2H (WD 1 ± 4%).

Both in WD patients and controls, S100A9(L) was detected only in the form oxidized at the cysteine residue: glutathionylated (WD 85 ± 16%, HC 98 ± 5%), cysteinylated (WD 7 ± 10%, HC 2 ± 5%), and dimeric (WD 8 ± 13%). Conversely, S100A9(S) was prevalently detected in the non-oxidized forms in WD patients (86 ± 24%), and HC subjects (80 ± 35%).

Discussion.

S100A8 and S100A9.

This study highlighted the higher level of S100A8, and S100A9 and their oxidized derivatives in saliva of WD patients with respect to controls. A different pattern of oxidation was observed for the two proteins, in particular at the cysteine residue: a) S100A8 was detected both reduced and oxidized at C42, while S100A9(L) was never detected with the reduced cysteine; b) S100A8 showed a major proneness with respect to S100A9(L) to irreversible oxidation of the cysteine residue, and sulfonic or sulfinic acid were the main oxidized derivatives of S100A8, while

S100A9 was detected principally glutathionylated, and to a minor extent cysteinylated and in the dimeric form.

S100A8, and S100A9 are the most abundant neutrophil proteins (about 45% of cytosolic proteins) constitutively expressed also by myeloid cells, platelets, and osteoclasts [34,35]. Several cell types (macrophages, monocytes, keratinocytes, fibroblasts) show an inducible strong expression of S100A8 and S100A9 in acute and chronic inflammatory, and oxidative stress conditions [35,36]. Interestingly, it has been reported that following liver damages, upregulated S100A8 and S100A9 induce neutrophils mobilization [37,38]. In activated granulocytes and macrophages, S100A8 and S100A9 are involved in the activation of NADPH oxidase 2 [39,40], and thus contribute to the generation of reactive oxygen/nitrogen/chlorine species (ROS/RNS/RCS) with a subsequent progression and exacerbation of the inflammatory status. Different factors, in addition to excess of unbound copper, can be responsible for WD redox unbalance, i.e. Hussain *et al.* observed an increased expression of the inducible nitric oxide synthase in WD [41], while Ogihara *et al.* demonstrated a decreased level of plasma antioxidants [42]. Furthermore, the decreased concentration of serum peroxiredoxin 2 isoform b was demonstrated in asymptomatic, early-stage WD patients [21]. Thus, the oxidative stress condition occurring in WD could be at the basis of the high concentration of S100A8 and S100A9 proteoforms observed in our patients, and the up regulation of S100A8 in WD patients should be responsible for the high levels of its oxidized forms, which however did not differ in percentage between patients and healthy controls.

S100A8 in the form of sulfonic, or sulfinic acid, or oxidized at M1, M78 and W54 residues, has been already observed *in vitro*, by treating recombinant S100A8 with HOCl, as well as *in vivo* in human asthmatic sputum [43], but the contemporaneous oxidation of C42 and the methionine

residues has not been observed. The present study not only highlighted that more oxidative modifications can co-occur in S100A8, but also showed that the hyper-oxidized derivatives represented the major proteoforms of S100A8 in saliva of both WD patients and controls.

Oxidation of cysteines to sulfinic and sulfonic acid is generally considered an irreversible modification, which damages the protein. However, the enzymatic reversion of the sulfinic acid to the thiol form has been also observed [44,45].

Reversible cysteine oxidation, such as glutahionylation, cysteinylation, and dimerization, can be involved in a variety of redox signaling/regulation events, and in the protection of critical cysteines from irreversible oxidative damages [46-48]. For instance, it has been reported that reversible cysteine oxidation of S100A8 and S100A9 can modulate their activity switching it from pro- to anti-inflammatory [35,43,49].

The present study reports for the first time the detection of S100A8-SSG *in vivo*. In a previous study, it has been demonstrated *in vitro* that both S100A9 and S100A8 can undergo glutathionylation via GSSG or GSNO intermediates, but only S100A9-SSG was detected *in vivo* in activated neutrophils [50]. Glutathionylation of S100A9 alters its capacity to form complexes with S100A8 (calprotectin), to bind endothelial cells, and limits neutrophil migration in inflammatory lesions. It has been suggested that this modification protects the protein from its oxidation to higher oligomers [50]. The great sensitivity to oxidation of S100A8 and S100A9 is in agreement with the detection in saliva of WD patients of disulfide-linked homo-S100A9(L) and hetero-S100A8/A9(L) dimers. The S100A9(L)-SSdimer was previously detected in the activated neutrophils [50], and similar modifications of human S100A8, and murin S100A8 and A9 were observed *in vitro* in the presence of HOCl, Cu^{2+} and /or H_2O_2 at low concentration

[51,52]. It has been reported that S100A8 disulfide-linked dimers do not exhibit chemotactic action [53].

pIgR fragments.

AVAD and ASVD peptides were found at high concentration in almost all the WD patients, while in 11/32 controls they were undetected. pIgR, a type I transmembrane glycoprotein playing the main role in the adaptive immune response on mucosal surfaces [54,55], transports polymeric IgA across mucosal epithelial cells. It is upregulated by pro-inflammatory cytokines, hormones and microbial factors, through a signaling pathway involving toll-like receptors 3 and 4 [55]. A proteolytic cleavage occurring in the glycosylated extracellular portion of pIgR generates the secretory component (19-603 residues), which has been detected also in human saliva [56]. The cleavage occurs by action of unknown proteases, probably released by activated neutrophils [55], and the highly conserved sequence 602-613 (PRLFAEEKAVAD) is believed to be the cleavage signal [54]. The AVAD peptide originates by a cleavage occurring in this region at the level of K609, and the ASVD peptide derives from AVAD by the trypsin-like cleavage at R622. The cleavage releasing the C-terminal glycine from both fragments could be made by several proteases, including cathepsins and matrix-metallopeptidases. AVAD and ASVD peptides do not derive from the secretory component, and have a sequence partially overlapped to the transmembrane portion (639-661) of pIgR. Thus, they should originate by degradation of pIgR after its release from disrupted cell membranes. The increased levels of the AVAD and ASVD observed in our patients may be a consequence of an increased disruption of cell membranes, due to the high production of ROS characteristic of WD. However, it cannot be excluded that pIgR itself may be increased in WD patients, even though conflicting data about pIgR levels and liver

diseases have been reported. For instance, high levels of pIgR have been associated to the invasion and metastasis of the hepatocellular carcinoma [57], while a down regulation of pIgR in intestinal mucosa of animal models subsequent to acute liver necrosis has been observed [58].

α-defensin 2 and 4.

WD saliva was characterized by the higher concentration of α-defensin 4 and α-defensin 2 with respect to controls. Unexpectedly, none variation of α-defensin 1 and 3 levels was observed, even if α-defensin 2 derives from their proteolytic cleavage [59]. Besides to antimicrobial activity, α-defensins can modulate the inflammatory responses through regulation of cytokine production [60,61]. This peptide, also called corticostatin, exhibits pro-inflammatory effects through its anti-corticotropin property, which inhibits the production of cortisol [62]. This property is intriguing, since it has been demonstrated that in humans and in other mammals glucocorticoids induce the metallothioneins, important intracellular copper storages [63,64]. High levels of α-defensin 4, therefore, can indirectly down-regulate the metallothioneins by contributing to increase the free copper, a feature not negligible in WD. From this point of view, it could be interesting to test metallothionein levels in WD patients in a future study.

Conclusions.

Due to the varied spectrum of manifestations and clinical features of WD, the diagnosis can be reached only by combining several clinical parameters. This study highlighted that the salivary proteome of WD patients reflects the oxidative stress and the inflammatory conditions characteristic of the pathology, signatures that could be useful diagnostic clues of disease exacerbation. The present findings encourage further investigation on a larger cohort of patients,

as well as on other pathologies involving the liver or the copper metabolism, in order to have suggestions on potential specific biomarkers of WD.

Acknowledgment.

The authors acknowledge the financial support of the Cagliari University; the Banco di Sardegna Foundation, Fin. 2013, project: “Studio pilota del proteoma salivare per l'individuazione di nuovi biomarcatori del Morbo di Wilson.”; Monica Sanna thanks Sardinia Regional Government for the financial support of her PhD scholarship (P.O.R. Sardegna F.S.E. Operational Programme of the Autonomous Region of Sardinia, European Social Fund 2007-2013 - Axis IV Human Resources, Objective l.3, Line of Activity l.3.1.); the Catholic University of Rome, the Italian National Research Council (CNR), and the Nando Peretti Foundation..

Abbreviations.

WD, Wilson’s disease; HC, healthy controls; XIC, extracted ion current; Mav., average mass value; PTMs, post-translational modifications; pIgR, polymeric immunoglobulin receptor; aPRPs, salivary acidic proline-rich proteins; -SNO, nitrosylated cysteine; -SSG, glutathionylated cysteine; -SSC, cysteinylated cysteine; -SSdimer, disulfide bridge dimer; -SO_2H, cysteine sulfinic acid; -SO_3H, cysteine sulfonic acid; -Wox, oxidized tryptophan; -Wdiox, dioxidized tryptophan; -Mox, methionine sulfoxide; 1P, monophosphorylated; S100A9(L), long S100A9; S100A9(S), short S100A9; AST, aspartate aminotransferase; ALT, alanina aminotransferase; ROS/RNS/RCS, reactive oxygen/nitrogen/chlorine species; SD, standard deviation.

References.

[1] Hellman NE, Kono S, Mancini GM, Hoogeboom AJ, De Jong GJ, Gitlin JD. Mechanisms of copper incorporation into human ceruloplasmin. J. Biol. Chem. 2002; 277:46632-8.

[2] Ala A, Walker AP, Ashkan K, Dooley JS, Schilsky ML. Wilson's disease. Lancet 2007; 369:397-408.

[3] Fanni D, Pilloni L, Orrù S, Coni P, Liguori C, Serra S, Lai ML, Uccheddu A, Contu L, Van Eyken P, Faa G. Expression of ATP7B in normal human liver. Eur. J. Histochem. 2005; 49:371-8.

[4] Huster D, Hoppert M, Lutsenko S, Zinke J, Lehmann C, Mössner J, Berr F, Caca K. Defective cellular localization of mutant ATP7B in Wilson's disease patients and hepatoma cell lines. Gastroenterology 2003; 124:335-45.

[5] Bugbee D, Davies L, Kenney S, Cox D. Dept. Med. Gen., Univ. Alberta, Canada. Wilson *Disease Mutation Database*. http://www.wilsondisease.med.ualberta.ca/database.asp (Accesed 2001).

[6] Wu F, Wang J, Qiao L, Jiang C. Wilson’s disease: a comprehensive review of the molecular mechanisms. Int. J. Mol. Sci. 2015; 16:6419-31.

[7] Gialluisi A, Incollu S, Pippucci T, Lepori MB, Zappu A, Loudianos G, Romeo G. the homozygosity index (HI) approach reveals high allele frequency for Wilson disease in the Sardinian population. Eur. J. Hum.Genet. 2013; 21:1308-11.

[8] Crisponi G, Nurchi VM, Gerosa C, Fanni D, Nemolato S, Faa G. Copper uptake and trafficking in the brain. In: Linert, W., Kozlowski, H., editors. Metal Ions in Neurological Systems. Wien: Springer; 2012, p. 47-63.

[9] Carta M, Mura G, Sorbello O, Farina G, Demelia L. Quality of Life and Psychiatric Symptoms in Wilson's Disease: the Relevance of Bipolar Disorders. Clin. Pract. Epidemiol. Ment. Health 2012; 8:102-9.

[10] Gitlin JD. Wilson disease. Gastroenterology 2003; 125:1868-77.

[11] Ferenci P, Caca K, Loudianos G, Mieli-Vergani G, Tanner S, Sternlieb I, Schilsky M, Cox D, Berr F. Diagnosis and phenotypic classification of Wilson disease. Liver Int. 2003; 23:139-42.

[12] Roberts EA, Schilsky ML. A practice guideline on Wilson disease. Hepatology 2003; 37:1475-92.

[13] Steindl P, Ferenci P, Dienes HP, Grimm G, Pabinger I, Madl C, Maier-Dobersberger T, Herneth A, Dragosics B, Meryn S, Knoflach P, Granditsch G, Gangl A. Wilson's disease in patients presenting with liver disease: a diagnostic challenge. Gastroenterology 1997; 113:212-8.

[14] Ferenci P, Steindl-Munda P, Vogel W, Jessner W, Gschwantler M, Stauber R, Datz C, Hackl F, Wrba F, Bauer, P, Lorenz O. Diagnostic value of quantitative hepatic copper determination in patients with Wilson's Disease. Clin. Gastroenterol. Hepatol. 2005; 3:811-8.

[15] Sini M, Sorbello O, Sanna F, Battolu F, Civolani A, Fanni D, Faa G, Demelia L. Histologic evolution and long-term outcome of Wilson's disease: results of a single-center experience. *Eur.* J. Gastroenterol. Hepatol. 2013; 25:111-7.

[16] Liggi M, Mais C, Demurtas M, Sorbello O, Demelia E, Civolani A, Demelia L. Uneven distribution of hepatic copper concentration and diagnostic value of double-sample biopsy in Wilson's disease. Scand. J. Gastroenterol. 2013; 48:1452-8.

[17] Lee BH, Kim JM, Heo SH, Mun JH, Kim J, Kim JH, Jin HY, Kim GH, Choi JH, Yoo HW. Proteomic analysis of the hepatic tissue of Long-Evans Cinnamon (LEC) rats according to the natural course of Wilson disease. Proteomics 2011; 11:3698-705.

[18] Simpson DM, Beynon RJ, Robertson DH, Loughran MJ, Haywood S. Copper-associated liver disease: a proteomics study of copper challenge in a sheep model. Proteomics 2004; 4:524-36.

[19] Wilmarth PA, Short KK, Fiehn O, Lutsenko S, David LL, Burkhead JL. A systems approach implicates nuclear receptor targeting in the Atp7b(-/-) mouse model of Wilson's disease. Metallomics 2012; 4:660-8.

[20] Roelofsen H, Balgobind R, Vonk RJ. Proteomic analyzes of copper metabolism in an in vitro model of Wilson disease using surface enhanced laser desorption/ionization-time of flight-mass spectrometry. J. Cell. Biochem. 2004; 93:732-40.

[21] Park JY, Mun JH, Lee BH, Heo SH, Kim GH, Yoo HW. Proteomic analysis of sera of asymptomatic, early-stage patients with Wilson's disease. Proteomics Clin. Appl. 2009; 3:1185-90.

[22] Zhang Z, Marshall AG. An universal algorithm for fast and automated charge state deconvolution of electrospray mass-to-charge ratio spectra. J. Am. Soc. Mass. Spectrom. 1998; 9:225–33.

[23] Castagnola M, Cabras T, Iavarone F, Vincenzoni F, Vitali A, Pisano E, Nemolato S, Scarano E, Fiorita A, Vento G, Tirone C, Romagnoli C, Cordaro M, Paludetti G, Faa, G,

Messana I. Top-down platform for deciphering the human salivary proteome. J. Matern. Fetal Neonatal. Med. 2012; 25:27-43.

[24] Messana I, Cabras T, Pisano E, Sanna MT, Olianas A, Manconi B, Pellegrini M, Paludetti G, Scarano E, Fiorita A, Agostino S, Contucci AM, Calò L, Picciotti PM, Manni A, Bennick A, Vitali A, Fanali C, Inzitari R, Castagnola M. Trafficking and postsecretory events responsible for the formation of secreted human salivary peptides: a proteomics approach. Mol. Cell. Proteomics 2008; 7:911-26.

[25] Cabras T, Pisano E, Mastinu A, Denotti G, Pusceddu PP, Inzitari R, Fanali C, Nemolato S, Castagnola M, Messana I. Alterations of the salivary secretory peptidome profile in children affected by type 1 diabetes. Mol. Cell. Proteomics 2010; 9:2099-108.

[26] Castagnola M, Inzitari R, Fanali C, Iavarone F, Vitali A, Desiderio C, Vento G, Tirone C, Romagnoli C, Cabras T, Manconi B, Sanna MT, Boi R, Pisano E, Olianas A, Pellegrini M, Nemolato S, Heizmann CW, Faa G, Messana I. The surprising composition of the salivary proteome of preterm human newborn. Mol. Cell. Proteomics 2011; 10, M110.003467.

[27] Castagnola M, Cabras T, Iavarone F, Fanali C, Messana I. Detection of Ca^{2+}-binding S100 proteins in human saliva by HPLC-ESI-MS. In: Heizmann C, editor. Methods in Molecular Biology, vol 963: Calcium-Binding Proteins and RAGE. New York: Springer protocols, Humana Press; 2013, p.357-71.

[28] Ong SE, Mann M. Mass spectrometry-based proteomics turns quantitative. Nat. Chem. Biol. 2005; 1:252-62.

[29] Messana I, Inzitari R, Fanali C, Cabras T, Castagnola M. Facts and artifacts in proteomics of body fluids. What proteomics of saliva is telling us? J. Sep. Sci. 2008; 31:1948-63.

[30] Cabras T, Pisano E, Boi R, Olianas A, Manconi B, Inzitari R, Fanali C, Giardina B, Castagnola M, Messana I. Age-dependent modifications of the human salivary secretory protein complex. J. Proteome Res. 2009; 8:4126-34.

[31] Cabras T, Melis M, Castagnola M, Padiglia A, Tepper BJ, Messana I, Tomassini Barbarossa I. Responsiveness to 6-n-propylthiouracil (PROP) is associated with salivary levels of two specific basic proline-rich proteins in humans. PLoS One 2012; 7:e30962.

[32] Shetty V, Spellman DS, Neubert TA. Characterization by tandem mass spectrometry of stable cysteine sulfenic acid in a cysteine switch peptide of matrix metalloproteinases. J. Am. Soc. Mass Spectrom. 2007; 18:1544-51.

[33] Wang Y, Vivekananda S, Men L, Zhang Q. Fragmentation of protonated ions of peptides containing cysteine, cysteine sulfinic acid, and cysteine sulfonic acid. J. Am. Soc. Mass. Spectrom. 2004; 15:697-702.

[34] Edgeworth J, Gorman M, Bennett R, Freemont P, Hogg N. Identification of p8, 14 as a highly abundant heterodimeric calcium binding protein complex of myeloid cells. J. Biol. Chem. 1991; 266:7706-13.

[35] Goyette J, Geczy CL. Inflammation-associated S100 proteins: new mechanisms that regulate function. Amino Acids 2011; 41:821-42.

[36] Carlsson H, Yhr M, Petersson S, Collins N, Polyak K, Enerbäck C. Psoriasin (S100A7) and calgranulin-B (S100A9) induction is dependent on reactive oxygen species and is downregulated by Bcl-2 and antioxidants. Cancer Biol. Ther. 2005; 4:998-1005.

[37] Moles A, Murphy L, Wilson CL, Chakraborty JB, Fox C, Park EJ, Mann J, Oakley F, Howarth R, Brain J, Masson S, Karin M, Seki E, Mann DA. A TLR2/S100A9/CXCL-2 signaling

network is necessary for neutrophil recruitment in acute and chronic liver injury in the mouse. J. Hepatol. 2014; 60:782-91.

[38] Wiechert L, Németh J, Pusterla T, Bauer C, De Ponti A, Manthey S, Marhenke S, Vogel A, Klingmüller U, Hess J, Angel P. Hepatocyte-specific S100A8 and S100A9 transgene expression in mice causes Cxcl1 induction and systemic neutrophil enrichment. Cell Commun. Signal. 2012; 10:40.

[39] Schenten V, Melchior C, Steinckwich N, Tschirhart EJ, Bréchard S. Sphingosine kinases regulate NOX2 activity via p38 MAPK-dependent translocation of S100A8/A9. J. Leukoc. Biol. 2011; 89:587-96.

[40] Doussiere J, Bouzidi F, Vignais PV. The S100A8/A9 protein as a partner for the cytosolic factors of NADPH oxidase activation in neutrophils. Eur. J. Biochem. 2002; 269:3246-55.

[41] Hussain SP, Raja K, Amstad PA, Sawyer M, Trudel LJ, Wogan GN, Hofseth LJ, Shields PG, Billiar TR, Trautwein C, Hohler T, Galle PR, Phillips DH, Markin R, Marrogi AJ, Harris CC. Increased p53 mutation load in nontumorous human liver of wilson disease and hemochromatosis: oxyradical overload diseases. Proc. Natl. Acad. Sci. USA 2000; 97:12770-5.

[42] Ogihara H, Ogihara T, Miki, M, Yasuda H, Mino M. Plasma copper and antioxidant status in Wilson's disease. Pediatr. Res. 1995; 37:219-26.

[43] Gomes LH, Raftery MJ, Yan WX, Goyette JD, Thomas PS, Geczy CL. S100A8 and S100A9-oxidant scavengers in inflammation. Free Radic. Biol. Med. 2013; 58:70-86.

[44] Biteau B, Labarre J, Toledano MB. ATP-dependent reduction of cysteine-sulphinic acid by S. cerevisiae sulphiredoxin. Nature. 2003; 425:980-984.

[45] Budanov AV, Sablina AA, Feinstein E, Koonin EV, Chumakov PM. Regeneration of peroxiredoxins by p53-regulated sestrins, homologs of bacterial AhpD. Science. 2004; 304:596-600.

[46] Martínez-Ruiz A, Cadenas S, Lamas S. Nitric oxide signaling: classical, less classical and nonclassical mechanisms. Free Radic. Biol. Med. 2011; 51:17-29.

[47] Hill BG, Bhatnagar A. Protein S-glutathiolation: redox-sensitive regulation of protein function. J. Mol. Cell. Cardiol. 2012; 52:559-67.

[48] Lindahl M, Mata-Cabana A, Kieselbach T. The disulfide proteome and other reactive cysteine proteomes: analysis and functional significance. Antioxid. Redox Signal. 2011; 14:2581-642.

[49] Sroussi HY, Lu Y, Villines D, Sun Y. The down regulation of neutrophil oxidative metabolism by S100A8 and S100A9: implication of the protease-activated receptor-2. Mol. Immunol. 2012; 50:42-8.

[50] Lim SY, Raftery MJ, Goyette J, Geczy CL. S-glutathionylation regulates inflammatory activities of S100A9. J. Biol. Chem. 2010; 285:14377-88.

[51] Kumar RK, Yang Z, Bilson S, Thliveris S, Cooke BE, Geczy CL. Dimeric S100A8 in human neutrophils is diminished after phagocytosis. J. Leukoc. Biol. 2001; 70:59-64.

[52] Harrison CA, Raftery MJ, Walsh J, Alewood P, Iismaa SE, Thliveris S, Geczy CL. Oxidation regulates the inflammatory properties of the murine S100 protein S100A8. J. Biol. Chem. 1999; 274:8561-9.

[53] Lim SY, Raftery MJ, Goyette J, Hsu K, Geczy CL. Oxidative modifications of S100 proteins: functional regulation by redox. J. Leukocyte Biol. 2009; 86:577-87.

[54] Asano M, Komiyama K. Polymeric immunoglobulin receptor. J. Oral Sci. 2011; 53:147-56.

[55] Kaetzel CS. The polymeric immunoglobulin receptor: bridging innate and adaptive immune responses at mucosal surfaces. Immunol. Rev. 2005; 206:83-99.

[56] Ramachandran P, Boontheung P, Xie Y, Sondej M, Wong DT, Loo JA. Identification of N-linked glycoproteins in human saliva by glycoprotein capture and mass spectrometry. J. Proteome Res. 2006; 5:1493-503.

[57] Ai J, Tang Q, Wu Y, Xu Y, Feng T, Zhou R, Chen Y, Gao X, Zhu Q, Yue X, Pan Q, Xu S, Li J, Huang M, Daugherty-Holtrop J, He Y, Xu HE, Fan J, Ding J, Geng M. The role of polymeric immunoglobulin receptor in inflammation-induced tumor metastasis of human hepatocellular carcinoma. J. Natl. Cancer Inst. 2011; 103:1696-712.

[58] Fu JL, Wang YR, Li GZ, Zhou Y, Liu P. Change in expression of the intestinal polymeric immunoglobulin receptor in acute liver necrosis. Journal of Gastroenterology and Hepatology Research 2012; 1:69-73.

[59] Valore EV, Ganz T. Posttranslational processing of defensins in immature human myeloid cells. Blood 1992; 79:1538-44.

[60] Chaly YV, Paleolog EM, Kolesnikova TS, Tikhonov II, Petratchenko EV, Voitenok NN. Neutrophil alpha-defensin human neutrophil peptide modulates cytokine production in human monocytes and adhesion molecule expression in endothelial cells. Eur. Cytokine Netw. 2000; 11:257-66.

[61] Lehrer RI, Lu W. α-Defensins in human innate immunity. Immunol Rev. 2012; 245:84-112.

[62] Singh A, Bateman A, Zhu QZ, Shimasaki S, Esch F, Solomon S. Structure of a novel human granulocyte peptide with anti-ACTH activity. Biochem. Biophys. Res. Commun. 1988; 155:524-9.

[63] Gedamu L, Foster R, Jahroudi N, Samson SL, Shworak NW, Zafarullah M. Regulation of human and rainbow trout metallothionein genes. In: Suzuki KT, Imura N, Kimura M, editors. Metallothionein II: Biological roles and medical implications. Basel: Berkhäuser Verlag; 1993, p.365-382.

[64] Miles AT, Hawksworth GM, Beattie JH, Rodilla V. Induction, Regulation, Degradation, and Biological Significance of Mammalian Metallothioneins Critical Reviews in Biochemistry and Molecular Biology 2000; 35:35–70.

CAPTIONS TO FIGURES

Figure 1. Typical low-resolution HPLC-ESI-MS profile of the acid soluble fraction of saliva from a WD patient, the elution range of several salivary proteins are indicated.

Figure 2. Flow-chart representing the approach utilized to analyze the salivary samples of WD patients and HC controls.

Figure 3. (A) High-resolution MS/MS analysis performed on the triply-charged ion with m/z 557.26 of the fragment 37-47 of S100A8-SSG. (B) High-resolution MS/MS analysis performed on the doubly-charged ion with m/z 877.93 of the tryptic peptide in which fragment 2-4 of S100A9(L) was linked to fragment 37-47 of S100A8.

Figure 4. Distribution of the XIC peak area values measured in saliva from WD and HC subjects of (A) S100A9(S), and S100A9(L)-SSG; (B) S100A8 and hyperoxidized S100A8 (S100A8-SO_3H/W_{54}-ox/M_{78}-ox or -SO_3H /W_{54}diox); (C) total S100A8ox and S100A9(L)ox; (D) α-defensins 2 and 4; (E) ASVD and AVAD peptides. Statistically significant differences are indicated with asterisks: *($p < 0.05$), **($p \leq 0.01$), ***($p \leq 0.001$).

Table1
Click here to download Table: Table_1.docx

Table 1. α-defensins, ASVD and AVAD peptides, S100A8 and S100A9 proteoforms, quantified in saliva of WD patients and controls. Swiss-prot code, elution time, experimental (Exp.) and theoretical (Th.) average and monoisotopic mass values (Mav., Mmonois.), and multiply charged ions used for XIC quantification are reported.

Protein (Swiss-Prot code)	**El. time (min)**	**Exp. Mav. (Th. Mav.) Da**	**Multiply-charged ions selected for the XIC procedures ($m/z_{(charge)}$)**	**Exp. Mmonois. (Th. Mmonois.) Da**
α-defensin 1 (P59665)	24.9-25.4	3442.1 ± 0.4 (3442.1)	$1722.0_{(+2)}$ $1148.4_{(+3)}$ $861.5_{(+4)}$	3439.53 ± 0.06 (3439.519)
α-defensin 2 (P59665 and P59666)	24.9-25.4	3371.0 ± 0.4 (3371.0)	$1686.5_{(+2)}$ $1124.7_{(+3)}$ $843.8_{(+4)}$	3368.49 ± 0.06 (3368.482)
α-defensin 3 (P59666)	24.9-25.4	3486.1 ± 0.4 (3486.1)	$1744.0_{(+2)}$ $1163.0_{(+3)}$ $872.5_{(+4)}$	3483.52 ± 0.06 (3483.509)
α-defensin 4 (P12838)	27.7-28.0	3709.3 ± 0.4 (3709.5)	$1855.7_{(+2)}$ $1237.5_{(+3)}$ $928.4_{(+4)}$	3706.78 ± 0.06 (3706.767)
AVAD (pIgR fr. 610-648 - P01833)	25.4-25.8	3834.4 ± 0.3 (3834.1)	$1918.0_{(+2)}$ $1279.0_{(+3)}$ $959.5_{(+4)}$	3831.85 ± 0.06 (3831.854)
ASVD (pIgR fr. 623-648 - P01833)	25.8-26.1	2490.5 ± 0.3 (2490.7)	$1246.3_{(+2)}$ $831.2_{(+3)}$	2490.23 ± 0.04 (2489.232)
S100A8 (P05109)	39.1-39.7	10833 ± 2 (10834.5)	$1355.3_{(+8)}$ $1204.8_{(+9)}$ $1084.5_{(+10)}$ $985.9_{(+11)}$	10827.8 ± 0.2 (10827.66)
S100A8-SO_2H	39.7-40.0	10866 ± 2 (10866.5)	$1359.3_{(+8)}$ $1208.4_{(+9)}$ $1087.7_{(+10)}$ $988.9_{(+11)}$	10859.6 ± 0.2 (10859.65)
S100A8-SO_3H/W54ox	40.2-40.6	10898 ± 2 (10898.6)	$1363.3_{(+8)}$ $1212.0_{(+9)}$ $1090.9_{(+10)}$ $991.8_{(+11)}$	10891.7 ± 0.2 (10891.66)
Hyperoxidized S100A8	39.0-39.6	10915 ± 2 (10914.6)	$1365.3_{(+8)}$ $1213.7_{(+9)}$ $1092.5_{(+10)}$ $993.2_{(+11)}$	10907.6 ± 0.2 (10907.63)
S100A8-SSG	38.1-38.4	11140 ± 2 (11139.8)	$1393.5_{(+8)}$ $1238.8_{(+9)}$ $1115.0_{(+10)}$ $1013.7_{(+11)}$	11133.8 ± 0.2 (11133.72)
S100A8-SNO	40.6-40.9	10863 ± 2 (10863.5)	$1358.9_{(+8)}$ $1208.1_{(+9)}$ $1087.3_{(+10)}$ $988.6_{(+11)}$	10856.6 ± 0.2 (10856.65)
S100A8/A9-SSdimer	41.6-41.9	23986 ± 3 (23985)	$1600.0_{(+15)}$ $1500.1_{(+16)}$ $1411.9_{(+17)}$ $1333.5_{(+18)}$ $1263.4_{(+19)}$ $1200.3_{(+20)}$ $1143.2_{(+21)}$ $1091.2_{(+22)}$ 1043.8(+23) 1000.4(+24) 960.4(+25) 923.5(+26)	nd[a]

S100A9(S) (P06702)	41.3-42.0	12690 ± 2 (12689.2)	$1410.9_{(+9)}$ $1269.9_{(+10)}$ $1154.6_{(+11)}$ $1058.4_{(+12)}$ $977.1_{(+13)}$	12681.4 ± 0.2 (12681.29)
S100A9(S) monophosphorylated	41.3-42.0	12770 ± 2 (12769.2)	$1419.8_{(+9)}$ $1277.9_{(+10)}$ $1161.8_{(+11)}$ $1065.1_{(+12)}$ $983.3_{(+13)}$	12761.1 ± 0.2 (12761.26)
S100A9(S)-Mox[b]	41.3-42.0	12706 ± 2 (12705.2)	$1412.7_{(+9)}$ $1271.5_{(+10)}$ $1156.0_{(+11)}$ $1059.8_{(+12)}$ $978.3_{(+13)}$	12697.4 ± 0.2 (12697.29)
S100A9(S)-Mox monophosphorylated	41.3-42.0	12786 ± 2 (12785.2)	$1421.9_{(+9)}$ $1279.5_{(+10)}$ $1163.3_{(+11)}$ $1066.4_{(+12)}$ $984.5_{(+13)}$	12777.2 ± 0.2 (12777.25)
S100A9(L)-SSG[c]	41.1-41.8	13459 ± 2 (13458.1)	$1346.8_{(+10)}$ $1224.5_{(+11)}$ $1122.5_{(+12)}$ $1036.3_{(+13)}$ $962.3_{(+14)}$	13449.7 ± 0.2 (13449.55)
S100A9(L)-SSG monophosphorylated	41.1-41.8	13539 ± 2 (13538.1)	$1354.8_{(+10)}$ $1231.8_{(+11)}$ $1129.2_{(+12)}$ $1042.4_{(+13)}$ $968.0_{(+14)}$	13529.3 ± 0.2 (13529.52)
S100A9(L)-SSG/Mox	41.0-41.6	13475 ± 2 (13474.1)	$1348.4_{(+10)}$ $1225.9_{(+11)}$ $1123.8_{(+12)}$ $1037.5_{(+13)}$ $963.4_{(+14)}$	13465.6 ± 0.2 (13465.55)
S100A9(L)-SSG/Mox monophosphorylated	41.0-41.6	13555 ± 2 (13554.1)	$1356.4_{(+10)}$ $1233.2_{(+11)}$ $1130.5_{(+12)}$ $1043.6_{(+13)}$ $969.1_{(+14)}$	13545.7 ± 0.2 (13545.52)
S100A9(L)-SSC[d]	41.1-41.8	13273 ± 2 (13271.9)	$1328.2_{(+10)}$ $1207.6_{(+11)}$ $1107.0_{(+12)}$ $1021.9_{(+13)}$ $949.0_{(+14)}$	13263.5 ± 0.2 (13263.49)
S100A9(L)- SSC monophosphorylated	41.1-41.8	13353 ± 2 (13351.9)	$1336.2_{(+10)}$ $1214.8_{(+11)}$ $1113.7_{(+12)}$ $1028.1_{(+13)}$ $954.7_{(+14)}$	13343.3 ± 0.2 (13343.46)
S100A9/A9-SSdimer	41.7-42.5	26306 ± 3 (26304)	$1754.6_{(+15)}$ $1645.0_{(+16)}$ $1548.3_{(+17)}$ $1462.3_{(+18)}$ $1385.4_{(+19)}$ $1316.2_{(+20)}$ $1253.5_{(+21)}$ $1196.6_{(+22)}$ $1144.6_{(+23)}$ $1097.0_{(+24)}$ $1053.1_{(+25)}$ $1012.7_{(+26)}$	nd

[a] nd: not determined; [b]Mox: methionine sulfoxide. [c]SSG indicates a glutathionylated cysteine residue. [d]SSC indicates a cysteinylated cysteine residue.

Table2
Click here to download Table: Table_2.docx

Table 2. Results of the high-resolution HPLC-ESI-MS/MS analysis of the oxidized tryptic peptides obtained by digestion of enriched fractions of S100A8 and S100A9 oxidized proteoforms**.** Experimental and theoretical monoisotopic $[M+H]^+$, time elution, sequence, PTM, and the multiply-charged ion used for MS/MS analysis of the peptides are reported.

Tryptic Peptides Exp. and (Th.) monois. $[M+H]^+$ Time elution (min)	**Sequence and position**	**PTMs**	**MS/MS analysis m/z and charge**
	S100A8		
2737.49 ± 0.04 (2737.48) (39.1)	mLTELEKALNSIIDVYHKYSLIK 1-23	M-sulfoxide	m/z 685.13 (+4)
1540.77 ± 0.03 (1540.77) (20.2)	KLLETEcPQYIR 36-47	C-sulfonic acid	m/z 770.89 (+2)
1540.77 ± 0.03 (1540.77) (18.5)	LLETEcPQYIRK 37-48	C-sulfonic acid	m/z 770.89 (+2)
1669.76 ± 0.03 (1669.76) (19.7)	LLETEcPQYIR 37-47	C-glutathionylation	m/z 557.25 (+3)
1412.68 ± 0.02 (1412.67) (20.2)	LLETEcPQYIR 37-47	C-sulfonic acid	m/z 706.84 (+2)
1396.68 ± 0.02 (1396.68) (19.9)	LLETEcPQYIR 37-47	C-sulfinic acid	m/z 698.84 (+2)
	S100A8/A9-SSdimer		
1754.86 ± 0.03 (1755.87) (19.5)	LLETEcPQYIR 37-47 (S100A8) ¦ Nα-Acet-TcK 2-4 (S100A9)	C-disulfide dimerization	m/z 585.62 (+3)
	S100A9		
1630.80 ± 0.03 (1630.80) (37.3)	QLSFEEFImLMAR 73-85	M-sulfoxide	m/z 815.90 (+2)
1630.80 ± 0.03 (1630.80) (32.7)	QLSFEEFIMLmAR 73-85	M-sulfoxide	m/z 815.90 (+2)
1758.82 ± 0.03 (1758.82) (18.3)	VIEHImEDLDTNADK 57-72	M-sulfoxide	m/z 879.91 (+2)
3354.61 ± 0.06 (3354.61) (35.8)	VIEHIMEDLDTNADKQLSFEEFImLMAR 57-85	M-sulfoxide	m/z 839.41 (+4)
2191.96 ± 0.04 (2191.96) (12.1)	mHEGDEGPGHHHKPGLGEGTP 94-114	M-sulfoxide	m/z 731.32 (+3)

Table3
Click here to download Table: Table_3.docx

Table 3. Results of statistical analysis for pIgR fragments, α-defensins 2-4, and proteoforms of S100A8, and S100A9. XIC peak area (mean ± standard deviation (SD), median x10^7, frequency) and the p value obtained by T-tests are reported for each peptide/protein.

Peptide/protein	**WD group Mean ± SD Median**	**Frequency**	**HC group Mean ± SD Median**	**Frequency**	**p value**
ASVD	1.1 ± 0.6 1.1	30/32	0.7 ± 0.7 0.5	21/32	0.02 ↑
AVAD	2.4 ± 1.2 2.2	31/32	1.3 ± 1.1 1.4	21/32	0.003 ↑
α-Defensin 2	9.3 ± 11.0 4.3	27/32	4.7 ± 5.1 2.7	25/32	0.04 ↑
α-Defensin 4	2.5 ± 2.8 1.2	24/32	0.8 ± 1.7 0.01	11/32	0.004 ↑
S100A9(S) (1P + non-P)	27.4 ± 30.4 14.8	27/32	9.6 ± 12.1 4.5	19/32	0.004 ↑
S100A9(S)-Mox (1P + non-P)	5.0 ± 8.0 1.4	16/32	2.4 ± 5.0 0.01	9/32	ns[a]
S100A9(L)-SSG (non-P)	15.9 ± 19.3 7.5	24/32	5.0 ± 7.6 0.01	15/32	0.007 ↑
S100A9(L)-SSC (1P + non-P)	2.3 ± 5.1 0.01	8/32	0.3 ± 1.5 0.01	3/32	ns
S100A9/A9-SSdimer	1.7 ± 4.6 0.01	5/32	0		na[b]
S100A8/A9-SSdimer	5.1 ± 13.8 0.01	5/32	0		na
S100A9(L)ox tot	28.6 ± 31.9 18.8	29/32	8.9 ± 13.4 1.9	15/32	0.006 ↑
S100A8	3.1 ± 4.7 0.01	15/32	0.5 ± 1.6 0.01	4/32	0.01 ↑
Hyperoxidized S100A8	3.0 ± 3.7 1.6	20/32	0.7 ± 1.6 0.01	7/32	0.002 ↑
S100A8-SO_3H/W54ox	1.1 ± 3.2 0.01	11/32	0.3 ± 0.8 0.01	5/32	ns
S100A8-SSG	0.5 ± 1.5 0.01	5/32	0		na
S100A8-SNO	2.7 ± 9.0 0.01	5/32	0		na
S100A8-SO_2H	0.3 ± 0.9 0.01	3/32	0		na

Peptide/protein	WD group Mean ± SD Median	Frequency	HC group Mean ± SD Median	Frequency	p value
S100A8ox tot	10.4 ± 14.8 4.3	23/32	0.9 ± 1.8 0.01	11/32	0.0003 ↑

[a]ns: not significant; [b]na: not applicable

Figure 1
Click here to download Figure: Figure_1.pptx

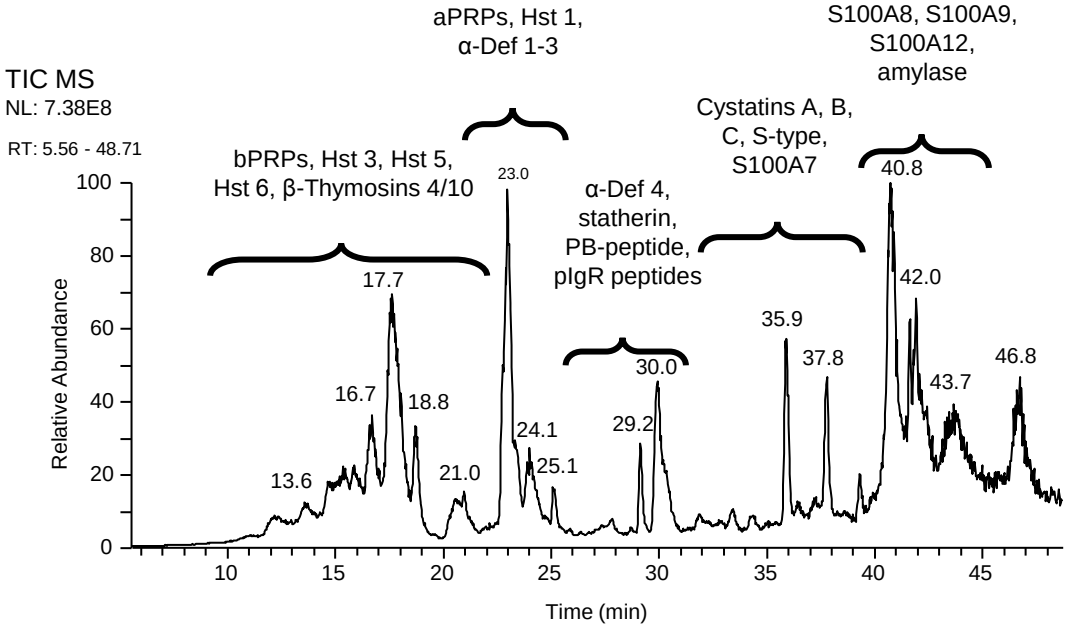

Figure 1

Figure 2
Click here to download Figure: Figure_2.pptx

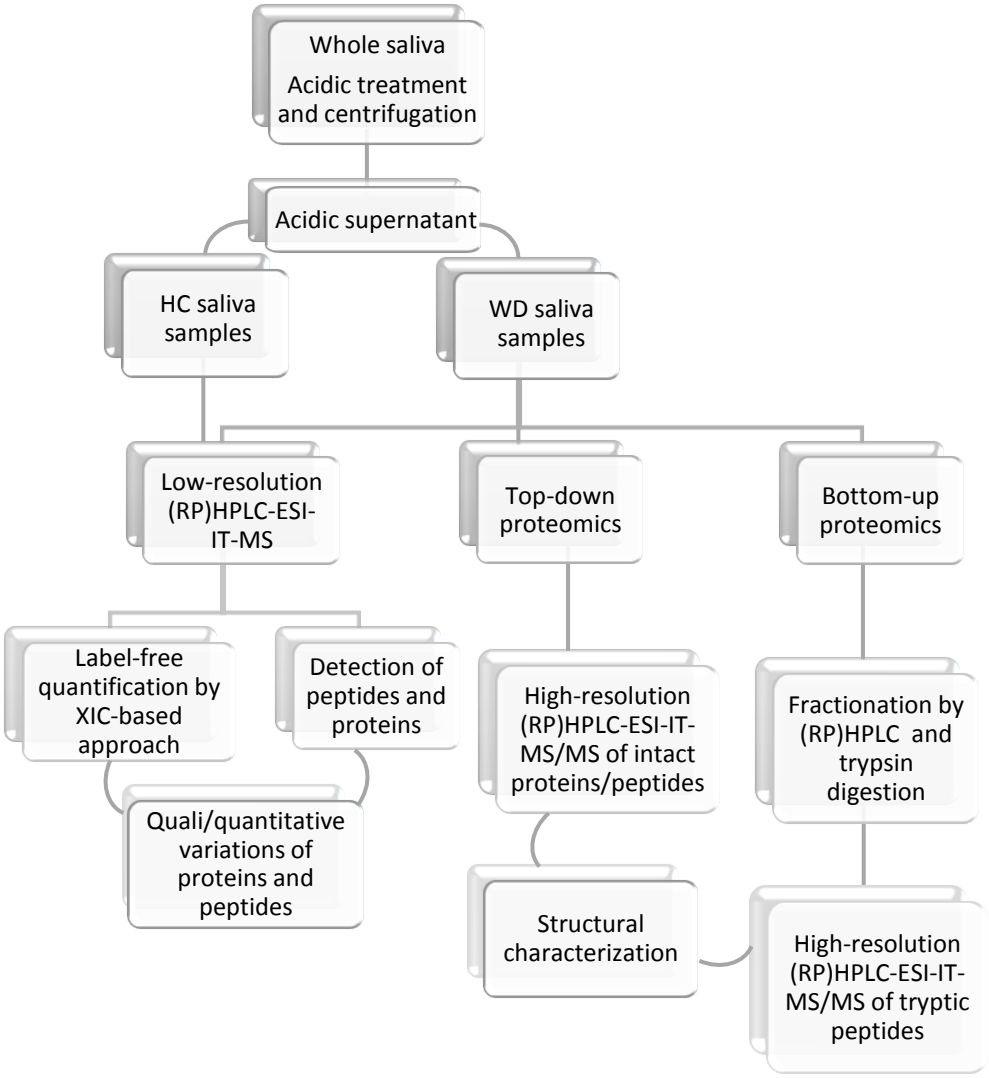

Figure 2

Figure 3

Click here to download Figure: Figure_3.pptx

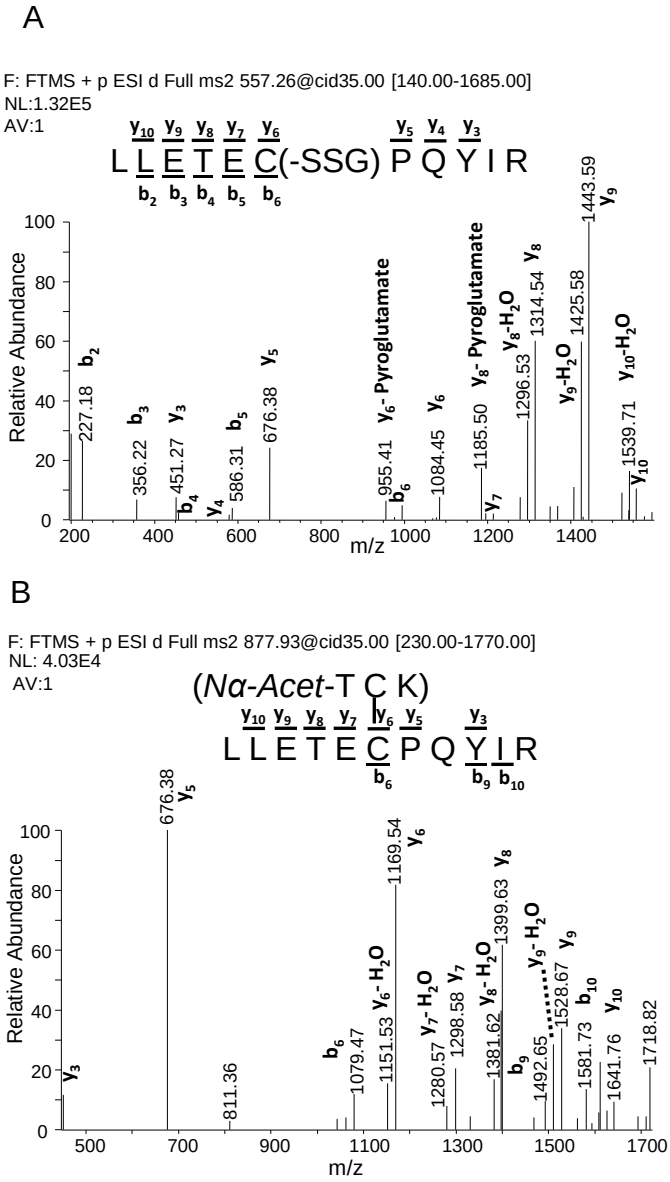

Figure 3

Figure 4
Click here to download Figure: Figure_4.pptx

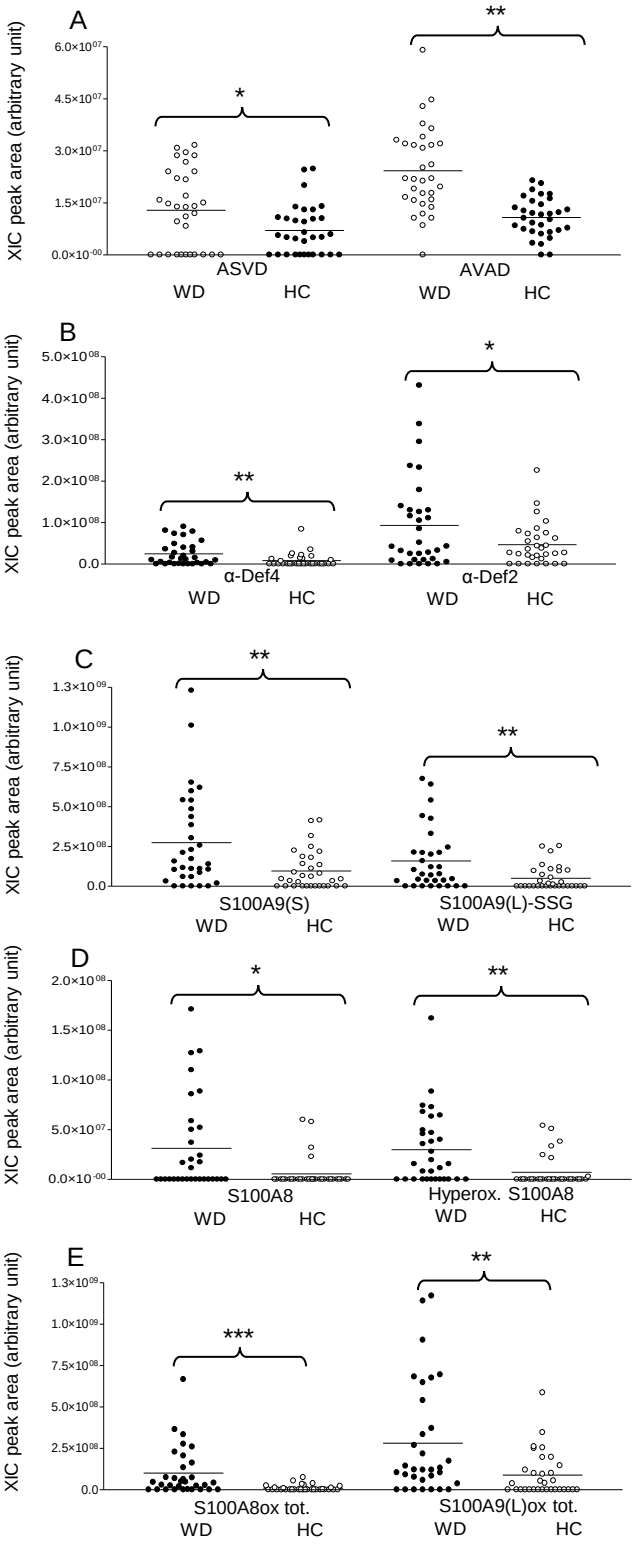

Figure 4

Supplementary material (Low_res_ESI-MS_method)

Click here to download Supplementary material: Low_res_ESI-MS_method.docx

Supplementary material (High_res_ESI-MS_method)

Click here to download Supplementary material: High_res_ESI-MS_method.docx

Supplementary material (Table S1)

Click here to download Supplementary material: Table S1.docx

Supplementary material (Top-down_proteomics_characterization)

Click here to download Supplementary material: Top-down_proteomics_characterization.docx

Supplementary material (Bottom-up_unmodified_S100A8-A9)

Click here to download Supplementary material: Bottom-up_proteomics_characterization_unmodified_S100A8-A9.docx

Supplementary material (Bottom-up_oxidized_S100A8-A9)

Click here to download Supplementary material: Bottom-up_proteomics_characterization_oxidized_S100A8-A9.docx

***Conflict of Interest**

Click here to download Conflict of Interest: Conflict of interest.docx